scientific reports

Check for updates

OPEN

Gamma oryzanol modulates hepatic lipids expression and regulates integrated pathways in liver disease pathophysiology under a high sugar fat diet

Juliana Silva Siqueira[1,2]✉, Camila Renata Correa[1], Gilda Aiello[2,3], Thiago Luiz Novaga Palacio[1], Jordanna Cruzeiro[1], Estela Oliveira Lima[1]✉, Hendrew Jesus Barbosa Campos de Souza[1], Fabiane Valentini Francisqueti-Ferron[4], Marina Carini[2], Giancarlo Aldini[2] & Alfonsina D'Amato[2]

Diets high in simple carbohydrates and saturated fats increase the risk of liver diseases. Gamma oryzanol (ORY), a compound found in rice bran, shows promise in addressing metabolic liver diseases, though its impact on lipid pathways requires further exploration. This study evaluated the effects of ORY in rats submitted to a high sugar-fat (HSF) diet using a multiomics approach to unravel its impact on lipid metabolism and associated pathways. Male Wistar rats were fed a control (CTRL), HSF, or HSF + ORY (0.5% w/w) diet for 30 weeks. Hepatic lipid profiling was performed using high-resolution mass spectrometry. Proteins and lipids were integrated into molecular pathway analyses. miR-122 expression was assessed by qRT-PCR, while oxidative stress markers were measured via colorimetric assays. The HSF diet altered 233 lipids compared to CTRL, while ORY supplementation modulated 84 lipids relative to the HSF group, with 39 lipids showing opposing regulatory profiles. Integrating proteomic data revealed key pathways in MAFLD pathophysiology affected by ORY. Additionally, ORY regulated miR-122 expression linked to lipid metabolism and reduced oxidative stress, demonstrating its potential to mitigate HSF-induced liver damage. ORY modulates hepatic lipid profiles and influences integrated metabolic networks, suggesting a significant role in MAFLD prevention and treatment.

Keywords Integratomics, Lipidomics, Steatosis, Phytosterol, Western diet

The liver, as an important metabolic organ, performs vital functions for the organism, among them orchestrating energy metabolism and acting on carbohydrate and lipid metabolism[1]. Under an obesogenic scenario, characterized by the consumption of diets rich in simple carbohydrates and saturated fat, the risk of liver diseases such as non-alcoholic fatty liver disease (NAFLD) and metabolic dysfunction-associated fatty liver disease (MAFLD) increases[2]. Gamma oryzanol (ORY), a bioactive compound found in rice bran oil, has shown antioxidant, anti-inflammatory and antilipidemic properties[3–5]. However, its specific effects on lipids and pathways within the organism remain poorly understood, limiting its potential as a therapeutic agent.

Emerging evidence suggests that specific lipid species, including diacylglycerols (DG), ceramides, and sphingomyelins (SM), play a role in the pathogenesis of MAFLD by modulating oxidative stress, inflammation, and mitochondrial function[6,7]. Oxidative stress contributes significantly to these processes by damaging lipids, proteins, and DNA, further accelerating the progression of liver diseases[8]. Consequently, canonical markers of lipid peroxidation and protein oxidation, including malondialdehyde (MDA) and carbonylated proteins (CBO), provide valuable biochemical indicators of these processes[9]. Additionally, miR-122, a liver-enriched microRNA, has been implicated as a central regulator of lipid metabolism and hepatic homeostasis, with its dysregulation linked to steatosis and inflammation[10–12].

[1]Botucatu Medical School, São Paulo State University (Unesp), Professor Montenegro Avenue, Botucatu 18618687, Brazil. [2]Department of Pharmaceutical Sciences, University of Milan, 20133 Milan, Italy. [3]Department for the Promotion of Human Science and Quality of Life, San Raffaele Open University, Milan, Rome, Italy. [4]Integrated Colleges of Buru (FIB), 17056100 Bauru, Brazil. ✉email: juliana.siqueira@unesp.br; estela.lima@unesp.br

The lipidomics approach enables a detailed characterization of lipid profiles and metabolic pathways involved in several diseases, particularly in liver, such as steatosis, cirrhosis and hepatocellular carcinoma[13]. Studies highlight the role of mitochondrial dysfunction in MAFLD progression, with distinct lipid species (e.g., cardiolipin, ubiquinone, SM) emerging as biomarkers and therapeutic targets[8,14,15]. Although lipidomics offers a comprehensive analysis of lipids, providing pathophysiological processes in various diseases, it offers a limited perspective. The integrative multiscale network of the interaction between lipid and protein can serve as early disease indicators, enabling more precise diagnosis and tracking of the disease progress. The integration of lipidomics and proteomics offers valuable insights into the pathogenesis and potential treatment strategies for NAFLD, highlighting the importance of a multi-omic approach in understanding complex diseases[13]. Furthermore, identifying these biomarkers opens new opportunities for therapeutic intervention, allowing the development of bioactive compounds that can act in a targeted and effective way to modulate these lipid pathways[13].

In a previous study, we comprehensively characterized the hepatic proteomic alterations induced by ORY supplementation in rats fed an HSF diet[5]. This proteomic analysis revealed that ORY modulated key metabolic pathways, including fatty acid β-oxidation, oxidative phosphorylation, and inflammatory signaling. Building upon these findings, the present study integrates novel lipidomic data with the previously published proteomic dataset to provide a more comprehensive understanding of how ORY influences hepatic lipid metabolism and the pathophysiological mechanisms underlying MAFLD progression. By combining these multi-omic approaches, this study aimed to investigate the effects of ORY in rats submitted to a high sugar-fat (HSF) diet to unravel its impact on lipid metabolism and associated pathways.

Results

Lipidome profiling and differential expression analysis

After normalization of the identified compounds, the lipidome profiles of each experimental condition were compared (Fig. 1). Differentially expressed lipids are displayed in the volcano plots. Red dots indicate up-regulation and blue dots indicate downregulation of the lipids. Among the 438 lipids identified, resulted from two-sided t-test (FC > 1.5, p-value < 0.05), there were 104 up-regulated and 129 down-regulated in the HSF group when compared to the CTRL group, belonging, in majority to diacylglycerols (DG; $n = 71$), phosphatidylcholines (PC; $n = 45$) and triacylglycerols (TG; $n = 26$) classes. Similarly, regarding the HSF + ORY/HSF groups comparison, 43 lipids are upregulated and 41 are downregulated, modulating, in majority, the DG ($n = 18$), PC ($n = 14$) and TG ($n = 17$) classes. The complete list of differentially expressed lipids observed in the volcanos is available in the supplementary Table 1 (ST1).

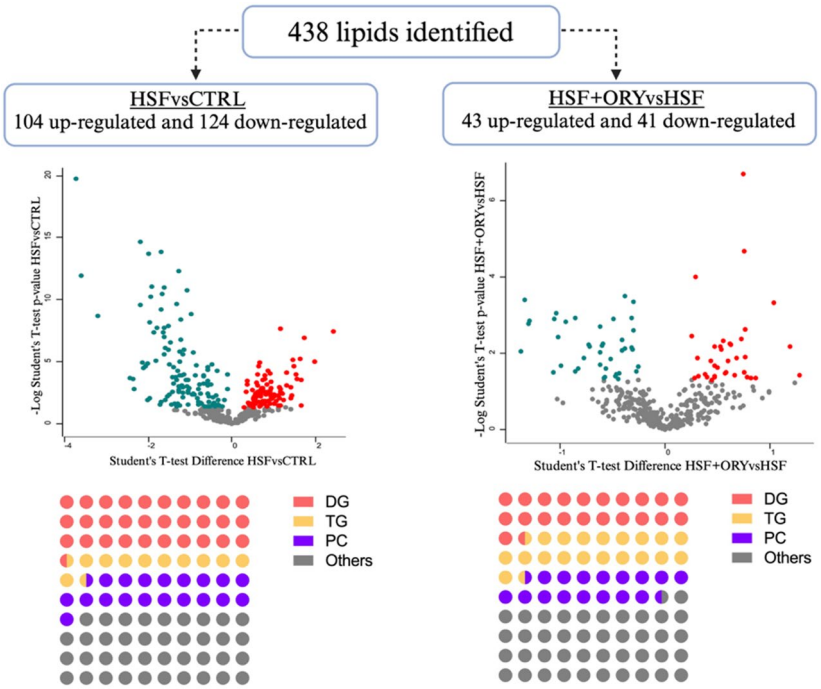

Fig. 1. Comparative Lipid Expression Profiles Across Groups. Volcano plots displaying the significance (-Log p-value) vs. difference highlighting the differentially expressed lipids in HSF/Control group and HSF + ORY/HSF group. Red dots indicate up-regulated lipids and green dots indicate down-regulated lipids. The bottom panel illustrates the major lipid classes significantly expressed, including diacylglycerols (DG), triacylglycerols (TG), phosphatidylcholines (PC), and others, with each class represented by a specific color. CTRL: Control; HSF: high sugar-fat; ORY: gamma-oryzanol. ($n = 6$/group). Created in BioRender. Siqueira, J. (2025) https://BioRender.com/r37r762.

The PLS-DA graph displays the distribution of samples in spaces defined by the first two discrimination components, with confidence ellipses representing the internal variability of each group. The clear distinction between groups indicates that the variables used in the PLS-DA model effectively discriminate between different experimental conditions (Fig. 2A). Additionally, Fig. 2B shows an evident separation between the control samples and those treated with HSF, highlighting the changes induced by the HSF treatment compared to the control group. The ellipse representing the HSF group partially overlaps with the ellipse of the HSF + ORY group, suggesting some similarities between the treatments while still maintaining a clear distinction between the two groups (Fig. 2C).

Commonly expressed lipids across experimental conditions

From differentially expressed lipids, the ones in common between the HSF/CTRL and HSF + ORY/HSF comparisons were identified (Table 1). Among the 39 lipids in common, in the HSF/CTRL comparison, 15 lipids were upregulated and 24 were downregulated. Conversely, in the HSF + ORY/HSF comparison, 23 lipids were upregulated while 16 lipids were downregulated.

Functional insights from multi-omics integration

Although independent proteomics and lipidomics analyses allow the understanding the pathophysiological pathways that developed in response to MAFLD and ORY supplementation, integrating them into a multi-omics description provides a deeper insight into its effects. The diseases and biofunctions associated to lipid molecules identified by UHPLC-HRMS during HSF administration and ORY supplementation using IPA software are presented in Table 2. The application of IPA software and its subsequent construction of a metabolic network have elucidated significant correlations between the consumption of an HSF diet and prevention with ORY, particularly in the context of lipid metabolism, inflammation, and cell viability. The nine subsets of lipids were highlighted for being involved in 163 networks related to liver disease: LPC 14:0 (*1–14:0 lysophosphatidylcholine*), LPC 16:0 (*1–16:0 lysophosphatidylcholine*), LPC 22:6 (*1–22:6(4Z,7Z,10Z,13Z,16Z,19Z) lysophosphatidylcholine*), LPE 16:0 (*1-palmitoyl-2-hydroxy-sn-glycero-3-phosphoethanolamine*), MG 20:4 (*2-arachidonoylglycerol*), NAE 20:4 (*anandamide*), PC 16:0_16:0 (*colfosceril palmitate*), NAE 18:0 (*N-stearoylethanolamine*), and CAR 18:0 (*stearoylcarnitine*).

In general, it has been observed that the consumption of the HSF diet has tended to be more prominently linked to pathways indicative of compromised lipid metabolism and subsequent hepatic damage, as opposed to the effects observed with ORY supplementation. The complete list of differentially expressed diseases and biofunctions observed is available in the supplementary table (ST2). Specifically, among the functional and disease modules identified, "cell death of hepatocytes" showed a positive z-score in the HSF group compared to

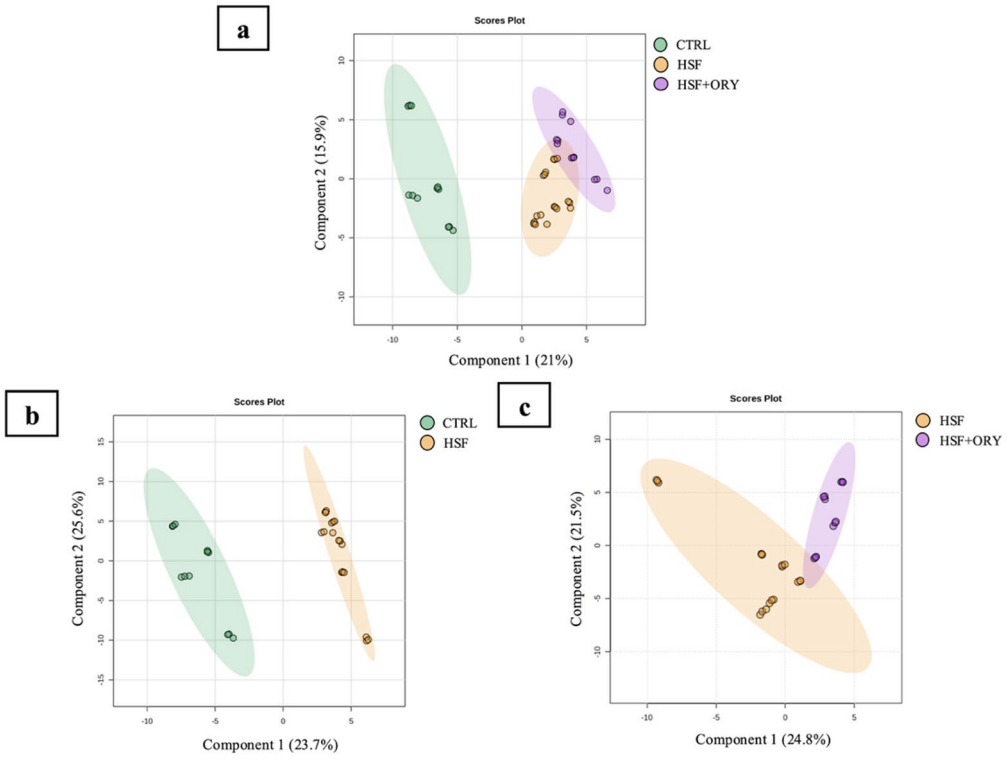

Fig. 2. Partial least square-discriminant analysis (PLS-DA) of the lipid profile in (**a**) CTRL, HSF and HSF + ORY groups, (**b**) CTRL and HSF groups, and (**c**) HSF and HSF + ORY groups. Each point in the plot corresponds to a liver sample replicate. CTRL: Control; HSF: high sugar-fat; ORY: gamma-oryzanol. ($n = 6$/group).

Metabolite name	HSFvsCTRL		HSF + ORYvsHSF	
	p-value	log2 ratio	*p*-value	log2 ratio
DG 26:3	1.25E-04	0.80	2.28E-02	−0.26
DG 34:3|DG 16:0_18:3	2.51E-02	−0.77	4.01E-02	−0.48
DG 36:0|DG 16:0_20:0	8.55E-05	0.92	8.26E-03	−0.31
DG 36:0|DG 18:0_18:0	8.55E-05	0.92	8.26E-03	−0.31
DG 36:4|DG 18:2_18:2	3.47E-05	−2.11	3.06E-02	−0.86
DG 36:5|DG 18:2_18:3	2.37E-05	−2.06	2.59E-02	−0.83
DG 38:0|DG 16:0_22:0	4.40E-03	0.69	4.56E-03	−0.42
DG 44:10	3.70E-08	2.42	9.45E-03	−0.63
LPC 18:3	6.39E-04	−0.68	6.15E-03	0.62
LPE 16:0	8.73E-04	−0.57	4.44E-02	0.28
LPE 22:6	3.87E-03	0.57	1.57E-02	0.43
MG 18:2	1.70E-04	−1.43	1.64E-02	0.60
MG 20:0	4.50E-02	−0.22	3.59E-03	0.25
NAE 16:1	2.75E-05	−0.57	2.61E-03	−0.31
NAE 18:2	4.13E-02	−0.57	8.74E-03	−0.41
NAE 20:5	1.29E-04	−1.20	6.24E-03	−0.61
PC 31:1	3.60E-03	−0.93	4.30E-02	0.40
PC 32:2|PC 14:0_18:2	8.46E-03	−0.83	3.42E-02	0.57
PC 32:2|PC 16:1_16:1	8.46E-03	−0.83	3.42E-02	0.57
PC 33:3	2.06E-15	−2.20	2.16E-05	0.75
PC 36:5|PC 18:2_18:3	1.84E-20	−3.72	3.17E-02	0.58
PC 36:6|PC 14:0_22:6	1.89E-02	−0.55	5.68E-03	0.61
PC 37:4|PC 17:0_20:4	1.92E-05	−0.86	3.12E-02	−0.27
PC 37:6|PC 15:0_22:6	3.25E-11	−1.66	4.16E-02	0.32
PC 40:9	6.55E-09	−1.97	3.81E-02	0.66
PC 41:6	1.65E-06	−1.24	1.54E-03	−0.95
PI 38:6	7.34E-04	−0.50	1.37E-02	0.31
PS 38:6	2.97E-04	−1.32	3.18E-02	0.75
SM 34:0;O2	3.34E-02	0.45	4.90E-02	−0.45
SM 36:1;O2|SM 18:1;O2/18:0	3.44E-02	0.51	6.80E-03	−0.73
ST 27:1;O	9.28E-04	−1.08	5.93E-03	−0.73
TG 36:0|TG 10:0_10:0_16:0	1.52E-03	0.73	4.31E-03	0.73
TG 36:0|TG 12:0_12:0_12:0	1.52E-03	0.73	2.47E-03	0.76
TG 46:1|TG 14:0_14:0_18:1	3.10E-02	0.41	8.04E-03	0.53
TG 46:2|TG 14:0_14:0_18:2	9.29E-03	0.51	4.75E-03	0.55
TG 46:2|TG 14:0_16:1_16:1	9.29E-03	0.51	4.75E-03	0.55
TG 48:1|TG 15:0_15:0_18:1	2.61E-02	0.92	4.41E-02	0.78
TG 48:1|TG 16:0_16:0_16:1	2.61E-02	0.92	4.41E-02	0.78
VAE 16:0	8.29E-12	−1.93	2.43E-02	0.50

Table 1. Commonly expressed lipids. DG: Diacylglycerol, LPC: Lysophosphatidylcholine, LPE: Lysophosphatidylethanolamine, MG: monoacylglyceride, NAE: N-acylethanolamine, PC: Phosphatidylcholine, PI: Phosphatidylinositol, PS: phosphatidylserine, SM: Sphingomyelin, ST: Sterol, TG: triacylglycerol, VAE: Vitamin A fatty acid ester, CTRL: Control, HSF: high sugar-fat, ORY: gamma-oryzanol.

the control group, (Figure. 3A). In contrast, this module exhibited a negative z-score in the HSF + ORY group relative to the HSF group, (Figure. 3B), highlighting its protective effect against hepatic damage.

Oxidative stress markers

The levels of MDA and CBO on the hepatic tissue are presented in Fig. 4. The HSF group had higher levels of lipoperoxidation and protein carbonylation when compared to the control group. ORY had a beneficial effect on preventing hepatic oxidative stress.

miR-122 and lipid metabolism regulation

The HSF diet caused a significant reduction in the relative expression of miR-122 in the liver of animals in the HSF group compared to the CTRL group, as shown in Fig. 5. Notably, supplementation with gamma oryzanol (ORY) counteracted this effect, significantly increasing the expression of miR-122 compared to the HSF group.

Functional Modules	Molecules (proteins and lipids)	HSFxCTRL		HSF + ORYxHSF	
		Z score	*p*-value	Z score	*p*-value
Accumulation of lipid	NAE 20:4. ABCB11, ACACA, ACADL, ACADVL, ACAT1, ACLY, ACOX1, […]	0.52	2,39E-12	−0.12	2,39E-12
Apoptosis	MG 20:4, NAE 20:4, ANXA2, ANXA4, ANXA5, ANXA6, APEX1, ARG1, […]	0.53	3,23E-16	−3.06	3,23E-16
Biosynthesis of polyunsaturated fatty acids	MG 20:4, NAE 20:4, ACACA, ACSL4, AKR1B1, ALB, ATP5PF, CBR1, […]	1.52	2,11E-06	0.99	2,11E-06
Catabolism of lipid	NAE 20:4, AADAC, ABAT, ACADL, ACADVL, ACAT1, ACOX1, ACSL1, […]	0.55	1,13E-13	2.4	1,13E-13
Cell death of hepatocytes	MG 20:4, NAE 20:4, ACSL4, ALDH2, CTH, CTNNB1, CTSB, DNM1L, […]	0.91	1,02E-05	−0.3	1,02E-05
Cell death of liver	MG 20:4, NAE 20:4, ACSL4, ALDH2, AMACR, C3, CTH, CTNNB1, […]	0.62	7,14E-08	−0.36	7,14E-08
Cell survival	NAE 20:4, AARS1, ABCC6, ABCE1, ACACA, ACLY, ACTN4, ACTR2, […]	1.18	1,32E-16	4.16	1,32E-16
Cell viability	NAE 20:4, AARS1, ABCE1, ACACA, ACLY, ACTN4, ACTR2, AHNAK, […]	1.68	3,02E-16	3.86	3,02E-16
Concentration of fatty acid	MG 20:4, NAE 20:4, ACACA, ACADL, ACADVL, ACLY, ACO2, ACOT13, […]	0.12	1,69E-25	1.47	1,69E-25
Inflammation of absolute anatomical region	LPC 14:0, LPC 16:0, LPC 22:6, LPE 16:0, MG 20:4, NAE 20:4, ABAT, ABCB11, […]	1.59	1,49E-13	−0.96	1,49E-13
Inflammation of body cavity	LPC 22:6, MG 20:4, NAE 20:4, ABAT, ABCB11, ABCC2, ACO2, ACOX1, […]	1.25	5,28E-13	−1.39	5,28E-13
Inflammation of liver	NAE 20:4, ABCB11, ABCC2, ACOX1, ADH4, AHNAK, ALB, APOB, […]	0.25	3,43E-08	0.06	3,43E-08
Inflammation of organ	LPC 14:0, LPC 22:6, LPE 16:0, MG 20:4, NAE 20:4, ABCB11, ABCC2, ACADVL, […]	1.3	1,14E-15	−1.07	1,14E-15
Liver lesion	LPC 14:0, MG 20:4, NAE 20:4, CAR 18:0, A1CF, AADAC, AADAT, AASS, […]	0.8	7,88E-34	0.03	7,88E-34
Metabolism of acylglycerol	MG 20:4, AADAC, ACSL1, ACSL4, ALDH1A1, APOA4, APOB, BHMT, […]	1.68	1,83E-08	0.48	1,83E-08
Metabolism of carbohydrate	MG 20:4, ACADM, ACP6, AGL, AKR1A1, AKR1B1, AKR1C4, AKR7A2, […]	0.98	1,38E-14	1.96	1,38E-14
Metabolism of polyunsaturated fatty acids	MG 20:4, NAE 20:4, NAE 18:0, ACACA, ACOX1, ACSL4, AKR1B1, ALB, […]	1.26	9,39E-12	1.64	9,39E-12
Necrosis of liver	MG 20:4, NAE 20:4, ACSL4, ALDH2, AMACR, C3, CTH, CTNNB1, […]	0.48	1,03E-07	−0.2	1,03E-07
Quantity of polyunsaturated fatty acids	MG 20:4, NAE 20:4, ACADVL, ACOT2, ACSL4, CD36, CYP1A2, Cyp2c23, […]	−0.02	6,12E-07	0.44	6,12E-07
Response of liver	NAE 20:4, ABCB11, ABCC2, ACOX1, ADH4, AHNAK, ALB, APOB, […]	0.06	5,84E-08	0.26	5,84E-08
Secretion of lipid	NAE 20:4, ABAT, ABCB11, ABCC2, ACADL, ACSL4, APOA4, APOB, […]	1.69	5,40E-06	1.19	5,40E-06
Synthesis of carbohydrate	MG 20:4, ACADM, ACP6, AKR1A1, AKR1B1, ALDH1A1, BSG, CD36, […]	0.47	1,56E-06	0.71	1,56E-06
Synthesis of fatty acid	MG 20:4, NAE 20:4, ABAT, ABCD3, ACACA, ACADL, ACADVL, ACAT1, […]	2.25	1,20E-16	2.04	1,20E-16
Synthesis of lipid	MG 20:4, NAE 20:4, ABAT, ABCB11, ABCD3, ACACA, ACADL, ACADVL, […]	1.65	5,76E-24	2.57	5,76E-24
Uptake of carbohydrate	LPC 14:0, ABCC2, ACLY, ACSL1, AIMP2, ALB, ANXA6, ARHGDIA, […]	1.74	1,51E-06	0.07	1,51E-06
Uptake of lipid	MG 20:4, NAE 20:4, ACSL1, APOA4, ATP11C, BSG, C3, CD36, […]	0.28	3,52E-07	1.2	3,52E-07

Table 2. Functional modules regulated by HSF diet and ORY prevention. 1–14:0 lysophosphatidylcholine: LPC 14:0; 1–16:0 lysophosphatidylcholine: LPC 16:0; 1–22:6(4Z,7Z,10Z,13Z,16Z,19Z) lysophosphatidylcholine: LPC 22:6; 1-palmitoyl-2-hydroxy-sn-glycero-3-phosphoethanolamine: LPE 16:0; 2-arachidonoylglycerol: MG 20:4; anandamide: NAE 20:4; colfosceril palmitate: PC 16:0_16:0; N-stearoylethanolamine: NAE 18:0; stearoylcarnitine: CAR 18:0; CTRL: control; HSF: high sugar-fat; ORY: gamma-oryzanol.

Discussion

Hepatic steatosis arises from the imbalance between the production and degradation of fatty acids, due to the overload of the liver's metabolic capacity associated with a high consumption of foods rich in sugars and fats, triggering changes in different dimensions. Untargeted integrated proteomics/lipidomics can act as a marker of hepatic dysfunction and a useful approach for functional investigations[13]. The ORY is known for its effect on chronic metabolic diseases and pathophysiological processes related to MAFLD[4]. Thus, this study is the first investigation into the impact of ORY on the hepatic integrated lipidome and proteome in rats subjected to an HSF diet.

The HSF diet provided to the experimental groups aims to mimic the Western diet, which, when consumed in excess, leads to metabolic diseases, such as MAFLD. As previously reported, animals consuming the HSF diet exhibited pronounced metabolic dysfunction compared to controls, including significant increases in final body weight, adiposity index, serum triglycerides, fasting glucose, insulin levels, and HOMA-IR, indicating the development of obesity, dyslipidemia, and insulin resistance[5]. Notably, supplementation with ORY was able to prevent weight gain and fat accumulation and significantly reduce triglyceride levels, fasting glucose, and insulin resistance markers. The anti-obesogenic effect of ORY is well-established by the literature, suggesting that the compound may play a role in regulating lipid metabolism and adipogenesis and potentially mitigating obesity-related processes and its associated comorbidities[4,5,16]. These findings highlight the promising potential of ORY as a natural compound in combating obesity and its associated health risks. Continued research into its mechanisms of action and long-term effects could provide valuable insights into its efficacy as a therapeutic agent in the fight against obesity.

A previous study demonstrated the effect of ORY on the protein profile in the liver in a diet induced NAFLD model[5]. Building upon this study, to provide a more comprehensive understanding of the potential pathways through which ORY acts, lipidomics analysis was performed and among all detected lipids several were differentially regulated. The highlighted subset of lipids is present between the HSF/CTRL and HSF + ORY/HSF comparisons and exhibits opposite expressions.

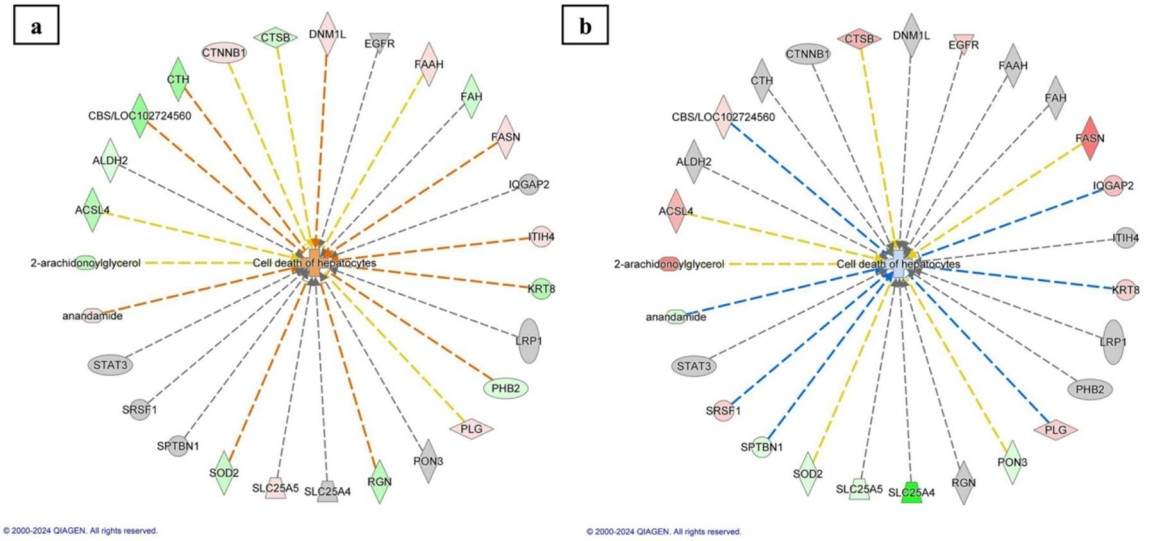

Fig. 3. Network Analyses of cell death of hepatocytes. (**a**) Cell death of hepatocytes between the HSF group in relation to the Control group. (**b**) Cell death of hepatocytes between the HSF + ORY group in relation to the HSF group. The orange and blue hubs indicate positive and negative-induced pathways, respectively. Gene up (red) or down (green) regulation is positively correlated with color intensity; orange and blue lines indicate activation and deactivation, respectively; yellow lines are designated for inconsistent findings; and grey lines represent unexpected not predicted effects. HSF: high sugar-fat, ORY: gamma-oryzanol.

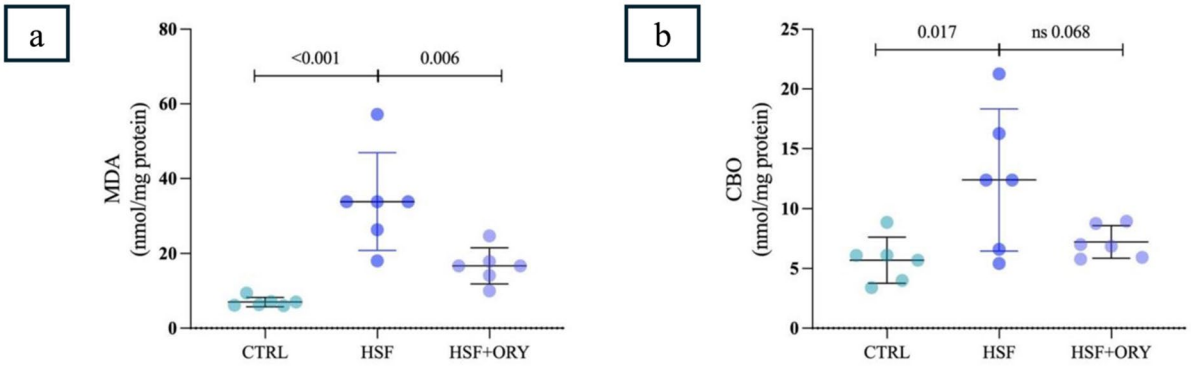

Fig. 4. Oxidative Stress Markers. (**a**) Malondialdehyde (nmol/mg protein). (**b**) Protein Carbonylation (nmol/mg protein). HSF: high sugar-fat, ORY: gamma-oryzanol. Values are shown as mean ± SD compared by one-way ANOVA followed by Tukey posthoc test, and differences were considered significant for $P < .05$ ($n = 6$/group).

Under normal conditions, the TG concentrations present in the liver are maintained by the balance between the rates of fatty acid accrual and removal. Excess fatty acids are retained in lipid droplets, a condition known as hepatic steatosis, one of the consequences of the spillover of dietary fatty acids from lipolysis of TG-rich lipoproteins[17]. Corroborating, the animals that consumed the HSF diet presented higher levels of hepatic TG when compared to the CTRL group. The harmful metabolic and lipotoxic effects of the hepatic steatosis may be due to the composition and incorporation of the hepatic lipids with other lipids species, such as, the most harmful effect of the incorporation of saturated and monounsaturated fatty acids (SFAs and MUFAs, respectively), when compared with polyunsaturated fatty acids (PUFAs). Therefore, the hepatic lipid profile of patients with hepatic steatosis is indicated by the enrichment of hepatic TG and DG with SFAs and MUFAs[17].

In general, elevated levels of DG is associated with the pathogenesis of metabolic disorders[18]. In the consumption of HSF diets, the DG participates in the synthesis of TGs, which can be accumulated in adipose tissue and are associated with the pathogenesis of obesity[17]. The liver and adipose tissue are closely linked, with adipocytes releasing free fatty acids and glycerol that can affect the formation and impact of DGs in the liver, which can vary in their effects on cellular signalling, insulin resistance, and hepatic steatosis[19]. The DGs can activate protein kinase C (PKC) isoforms and induce the expression of signalling pathways such as nuclear factor kappa B (NF-kB) and transforming growth factor beta (TGF-β). Specifically, the DGs can inhibit the tyrosine kinase activity of the insulin receptor through PKC-ε activity, compromising insulin signalling and

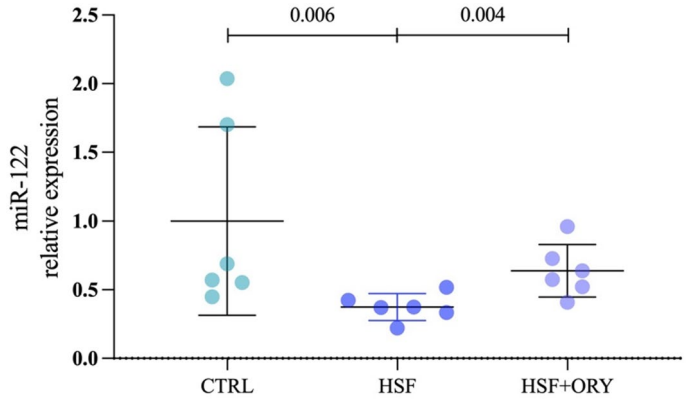

Fig. 5. miR-122 relative expression. HSF: high sugar-fat, ORY: gamma-oryzanol. Values are shown as mean ± SD compared by one-way ANOVA followed by Tukey posthoc test, and differences were considered significant for $P < .05$ ($n = 6$/group).

consequently leading to insulin resistance[20]. Further, in a mice model of a high-fat diet, the deletion of the gene encoding PKC-ε couldn't induce insulin resistance despite an increase in hepatic TG contents[21]. That said, it was possible to observe that the HSF group exerts an increased content in DGs containing SFAs in relation to the CTRL group. On the other hand, the ORY supplementation was able to decrease the hepatic DG contents when compared to the HSF group, which is consistent with the observed improvements in insulin resistance markers (e.g., HOMA-IR) in ORY-supplemented animals.

Meanwhile, PC are the main component of dietary phospholipids and provide a wide range of physiological effects, participating as a precursor of signalling molecules[22]. Hepatic TGs are accumulated in animal models of defective PC biosynthesis due to impaired VLDL secretion[17]. The reduction of PCs levels in the HSF group may be due to the cleavage of the PC moiety through the PC-phospholipase that releases DG and, consequently, contributes to the increase of TG synthesis and the subsequent development of steatosis[23]. In contrast, the ORY supplementation was able to improve the hepatic PCs content in relation to the HSF group. The PCs act as ligands of peroxisome proliferator-activated receptor-α (PPAR-α), a major regulator of energy homeostasis[24]. Consistent with prior published studies, the ORY molecule acts as an agonist, promoting anti-obesogenic effects and mitigating insulin resistance through PPAR-α stimulation[25].

In addition, the transfer of a phosphocholine headgroup from PC to ceramide produces DG and SM. The SM is a type of sphingolipid, a structural lipid and potent signalling molecule essential for cell growth and survival[26]. The HSF group demonstrated an elevation in SM levels compared to the CTRL group. The increased levels of saturated SM are associated with the pathogenesis of NAFLD, being positively correlated to levels of some hepatic enzymes, such as aspartate aminotransferase and alanine aminotransferase, in fatty liver and insulin resistance in animal models[27]. The reduction of SM synthesis, by a liver specific SM synthase-2 (SMS-2) has been associated with beneficial effects like decreased fat accumulation, inflammation and liver fibrosis[28]. Corroborating, our study found that ORY supplementation lowered significantly SM levels compared to the HSF group. Interestingly, knockout SMS-2 mice fed with a high-fat diet did not present insulin resistance, characterized by decreased expression of the insulin receptor and adiponectin[27]. This result aligns with existing research demonstrating that hepatic expression of adipoR2, a key adiponectin receptor in the liver, is decreased in obese mice. Furthermore, previously studies showed that ORY supplementation has the capacity to upregulate the AdipoR2/PPAR-α axis[25]. Taken together, findings suggest that ORY may supress SM levels and activate the Adipo-R2/PPAR-α pathway, contributing to its potential benefits in reducing fat accumulation, inflammation, and liver fibrosis.

In parallel, the classical oxidative stress markes further corroborated the multi-omic findings. MDA, a well-established marker of lipid peroxidation, reflects membrane damage and excessive reactive oxygen species production, while CBO represents protein carbonylation, an irreversible oxidative modification linked to impaired enzyme function and mitochondrial dysfunction[29]. Both markers were significantly elevated in the HSF group, consistent with the lipotoxic lipid profile and the proteomic evidence of disrupted mitochondrial and antioxidant pathways[5]. ORY supplementation prevented these increases, suggesting that its beneficial effects are not limited to lipid remodelling, but also extend to the attenuation of oxidative stress. The inclusion of MDA and CBO markers therefore provides biochemical validation of the omics results, reinforcing the integrative view of ORY as a modulator of lipid metabolism, redox balance, and hepatic function[30].

The results also reveal the potential relevance of miR-122 in modulating alterations observed in this MAFLD model. Previous studies have identified miR-122 as a key microRNA, due to its hepatocyte-specific expression and central role in regulating key lipogenic and fatty acid oxidation pathways, making it an integrative marker of lipidomic and proteomic alterations observed in this study[31]. The reduction of miR-122 in obese animals has been associated with increased lipid synthesis and the progression of hepatic steatosis, corroborating our findings. On the other hand, the increase in miR-122 levels in animals treated with ORY suggests an integrative link between classical biomarkers, lipidomic alterations, and proteomic pathways. Literature reports indicate that miR-122 regulates targets such as SREBP-1c, ACC1, FASN, and PPAR isoforms, which are key nodes in hepatic

lipid metabolism[32,33]. The restoration of miR-122 expression by ORY could contribute to the downregulation of lipogenic pathways and the activation of PPAR-α- related fatty acid oxidation, consistent with the observed decreases in DG and SM and the recovery of PC levels. These data point to miR-122 as an integrative mediator that enriches the biological interpretation of our multi-omic data and enhances the understanding of ORY's hepatoprotective effects.

In order to go deeper into the mechanisms underlying the identified lipids physiological and pathological impacts, we integrated the proteomic previously published findings with the lipidomic analysis[5]. The integration of lipidomic and proteomic data, summarized in Table 2; Fig. 3, highlights how specific lipid mediator converge with protein networks to modulate hepatocellular outcomes. The IPA network predicted some functional modules related to lipid metabolism, inflammatory response, and cell viability. Notably, NAE 20:4 (anandamide), MG 20:4(2-arachidonoyglycerol), and LPC 14:0 emerged as the most relevant lipids, being implicated in 101,100 and 36 pathways, respectively. These molecules were consistently mapped to modules associated with apoptosis, necrosis, and inflammation, with positive z-scores in the HSF group and inverse regulation with ORY supplementation, indicating their central role in the integrated response.

NAE 20:4 and MG 20:4 are endocannabinoids that play crucial roles in the endocannabinoid system, which was recently recognized as a potential target for obesity metabolic complication due to its participation on regulation of energy balance[34]. NAE 20:4 and MG: 20:4 are hydrolysate by specific enzymes, named as fatty acid amide hydrolase (FAAH) and monoacylglycerol lipase (MAGL), respectively[35]. Pharmacological inhibition of FAAH in diet-induced obesity models worsens metabolic outcomes[34]. Previous studies report that NAE 20:4 preferentially binds to CB1 receptor, promoting SREBP1-c- driven lipogenesis and inhibiting AMPK activity, thereby reducing fatty acid oxidation[35,36]. In contrast, MG 20:4 can activate both CB1 and CB2 receptors, and CB2 signalling has been associated with hepatocyte survival and regeneration in models of liver injury[37]. In agreement with these mechanistic insights, our data showed increased hepatic NAE 20:4 and reduced MG 20:4 in the HSF groups, whereas ORY supplementation reversed this pattern. Although we did not directly evaluate SREBP-1c or AMPK in this study, these lipidomic changes are consistent with previously reported CB1 and CB2 mediated effects and with the proteomic alterations observed in pathways related to fatty acid metabolism and cell survival[5,25,38]. These lipid changes are paralleled by coordinated proteomic alterations in cell death-related proteins, linking endocannabinoid signalling directly to hepatocyte survival and apoptosis pathways.

Proteomic integration revealed coordinated changes in key cell death-related proteins, complementing these lipid alterations. ACSL4 and CTSB were downregulated in HSF in relation to the CTRL group, while ORY partially restored their levels, suggesting improved fatty acid metabolism and reduced susceptibility to lipotoxicity-induced apoptosis and necrosis[39,40]. Antioxidant defences were also modulated, with SOD1 markedly decreased in HSF and elevated with ORY, whereas SOD2 remained suppressed in HSF but unchanged by ORY, reflecting partial restoration of redox balance[41]. PHB2 showed a slight decrease in HSF with no effect of ORY, indicating subtle modulation of mitochondrial stability. These integrated changes highlight the coordinated impact of ORY on hepatocyte survival, linking endocannabinoid signaling with regulation of apoptosis pathways and reinforcing its protective effects.

Moreover, the increased hepatic lipid influx in high-fat ingestion promotes a priority on oxidizing fatty acids to obtain energy, increasing mitochondrial activity. However, when this process becomes chronic, it eventually induces hepatic oxidative stress that contributes to decreased mitochondrial activity[8]. During fatty acid oxidation, the damaged mitochondria produce higher levels of lipotoxic intermediates, such as ceramides, DGs, and LPC[17], which contribute to insulin resistance by impairing the function of Insulin Receptor Substrates (IRS) proteins. A high concentration of free fatty acids also activates Type 4 Toll-like receptors (TLR-4), which impair the phosphorylation of IRS-1, also contributing to insulin resistance[17]. Moreover, inflammation is recognized as a key driver of multiorgan failure and death in liver disease[19]. The LPCs play distinct roles in regulating inflammation, with both pro-inflammatory and anti-inflammatory effects noted in various diseases[19]. LPC species were also identified as key regulators in IPA modules associated with inflammation and liver injury. Proteomic integration highlighted relevant inflammatory mediators, such as MYH6, which was strongly up-regulated in HSF and markedly down-regulated with ORY supplementation, and has been previously associated with systemic metabolic regulation and lipid utilization through cardiac-hepatic crosstalk, linking LPC alterations to inflammatory and necrotic signalling pathways[42]. In addition, higher levels of LPC 20:4 and LPC 22:6 have been reported in HSF diet models and before liver fibrosis progression in liver disease, respectively, indicating that these LPCs may be a biomarker for the stage of NAFLD progression[19]. Corroborating these findings, our results show that the levels of LPC 14:0, LPC 16:0 and LPC 22:6 were up regulated in the HSF group when compared to the CTRL group. Mechanistically, LPCs can activate TLR-4 and promote NF-κB mediated inflammasome signalling, involving HMGB1-NLRP3 activation[2,43]. Therefore, the observed reduction of LPC species with ORY supplementation may indirectly point to an attenuation of pro-inflammatory signalling cascades and cell death, as supported by previous studies. Furthermore, miR-122 may act as an integrative mediator linking these lipidomic and proteomic changes, influencing downstream pathways related to lipid metabolism, mitochondrial function, and oxidative stress, and thereby reinforcing the coordinated hepatoprotective effects of ORY.

In sum, the integration of these findings highlights the complex role of ORY in disease modulation and points to its potential as a therapeutic agent in the prevention and management of MAFLD characterized by dysregulated lipid metabolism, chronic inflammation, and compromised cell viability. This study provides an in-depth exploratory analysis of the hepatic lipidomic and proteomic alterations induced by ORY in a model of HSF diet-induced metabolic MAFLD. While our findings highlight key pathways modulated by ORY, further research is required to elucidate the precise molecular mechanisms involved in its hepatoprotective effects. Future studies should incorporate mechanistic approaches, such as targeted inhibition or activation of specific pathways, to validate the functional relevance of the observed lipid and protein alterations. While the current study provides robust insights, it is worth noting that the sample size was modest ($n = 6$ per group). Additional studies with larger

cohorts may confirm these results and strengthen statistical power. Furthermore, the translational applicability of ORY should consider potential dose-dependence, species differences, and bioavailability. In this study, ORY was administered via diet at 0.5%, corresponding to approximately 50 mg/day per animal, based on their daily consumption, a dose comparable to that used in clinical studies demonstrating safety and beneficial effects on systemic lipid metabolism[44]. Although this dosage was effective in modulating lipid and protein alterations, human translational may be influenced by factors such as dose-dependence, bioavailability, and interspecies differences. Clinical evidence suggests that ORY is generally well tolerated yet optimal dosing strategies and pharmacokinetics require further investigation to maximize efficacy[45]. The insights gained from this work can serve as a valuable reference for researchers seeking to investigate the detailed mechanistic role of ORY in hepatic metabolism and its potential therapeutic applications. Addressing this gap will enhance the translational applicability of these findings and provide a more comprehensive understanding of ORY's therapeutic potential.

Materials and methods

Animal model and experimental protocol

This study was conducted in accordance with the ARRIVE guidelines (https://arriveguidelines.org) to ensure high standards in the reporting of animal research. All procedures were approved by the Ethics Committee on Animal Experiments of the Botucatu Medical School, São Paulo State University, UNESP (protocol no. 1451/2024-CEUA), and followed the Guide for the Care and Use of Laboratory Animals. The nature of the procedures was evaluated by the institutional committee and classified as experimental. All clinical and handling procedures were carried out in accordance with institutional standard operating procedures and national regulations for animal research.

We used the animals and materials from a previously published study[5]. Briefly, Wistar rats ± 187 g from the Central vivarium of the São Paulo State University in Botucatu were housed in individual cages under a 12 h light-dark cycle at a room temperature of 24 °C ± 2 °C and humidity with water and food *ad libitum*. The animals were randomly assigned to three experimental groups (n = 6/group): the control (CTRL) group, receiving a standard diet; the HSF group, that received a HSF chow plus 25% of sucrose added to the drinking water; and the HSF plus supplementation with ORY (HSF + ORY), receiving the compound added to the HSF chow at the dose of 0.5% (w/w) and 25% of sucrose added to the drinking water. An additional group receiving a control diet supplemented with ORY was included to assess food, water, and calorie intake. These data are provided in Supplementary Table 3 (ST3). The diets composition and ORY dose were based on previously published studies[4,5,46–48]. After 30 weeks the animals were fasted for 8 h, anesthetized (300 mg/kg ketamine; 30 mg/kg xylazine; i.p.), and euthanized by decapitation. The liver was excised, weighed and immediately frozen in liquid nitrogen and stored at −80 °C for subsequent analysis.

Comprehensive nutritional, metabolic, and histological assessments, including caloric intake, final body weight, adiposity index, insulin resistance markers (HOMA-IR, TyG index), intrahepatic triglyceride content, and liver histology were performed and have been previously described in detail[5].

Untargeted lipidomics analysis

Lipid extraction

The lipids extraction was performed by the standard methyl tert-butyl ether (MTBE) protocol (Fig. 6A)[49]. All solvents used for the extraction contained 0.1%BHT (w/v). Briefly, left lobe liver samples ± 30 mg per group was homogenized by glass beat beating (3 cycles, 60", 350 rpm) in 300µL of isopropanol and water (i-PrOH: H_20, 50:50, v: v). After centrifugation (4000 rpm, 4 °C for 10 min), an aliquot was taken for BCA protein assay. An aliquot corresponding to 80 µg was quickly spiked with 5 µl of SPLASH® LIPIDO-MIX® (Avanti Polar Lipids Inc.- Alabaster, AL, USA, #330707) and left into ice for 15 min. The pooled quality control (QC) was prepared with aliquots corresponding to 08 µg of all samples. The protocol containing MTBE/methanol/water (4:1.2:1, v: v:v) was used as extraction solvents ratio. After adding the MTBE and methanol the samples were vortexed and incubated for 1 h at 4 °C on orbital shaker. Later, the water was added and a new incubation of 10 min at 4 °C in a horizontal shaker was performed. The samples were then centrifuged (10000 rpm, 4 °C for 10 min) and the upper phase was collected and dried under vacuum (Eppendorf concentrator 5301). Dried aliquots were stored at −80 °C and dissolved in 100µL in H_2O: Acetronitrile (H_2O: ACN, 60:40, v: v) with ammonium acetate and 0.1% formic acid, and vortexed before LC-MS/MS analysis.

Mass spectrometry (UHPLC-HRMS)

Lipid were separated using reverse phase chromatography on a HPLC Ultimate 3000 (Thermo Fisher Scientific, Bremen, Germany) equipped with an Accucore C18 column (150 × 2.1 mm; 2.6 µm, 150 Å; Thermo Fisher Scientific, Bremen, Germany). Gradient elution with solvent A (H_2O/ACN, 60:40, v/v) and B (i-PrOH: ACN, 90:10, v/v), both containing 10 mM ammonium acetate and 0.1% formic acid (v/v). A flow rate of 300 µL/min was used. The column and autosampler temperatures were set at 45 °C and 15 °C, respectively. The sample injection volume was 25 µL. The following gradient profile was used: 0.00 min, 45% B; 2.00 min, 45% B; 30.00 min, 97% B; 38.00 min, 97% B; 38.10 min, 45% B; 40.00 min, 45% B. MS spectra were collected over an m/z range of 140–1500 Da, operating in IDA® mode (Information Dependent Acquisition). The collision energy was set at 35 (CES 15). The polarity was ESI positive. Three technical replicates (LC-MS/MS runs) were performed. QC samples were run at the beginning of the sequence, during the sequence, and at the end of the sequence. MS-DIAL software (RIKEN, version 4.90, https://systemsomicslab.github.io/compms/msdial/main.html) was used to process the MS data[49]. This involved peaks detection, MS2 data deconvolution, alignment of peaks through all the samples and lipid identification. For which a cut-off value of 80% was selected.

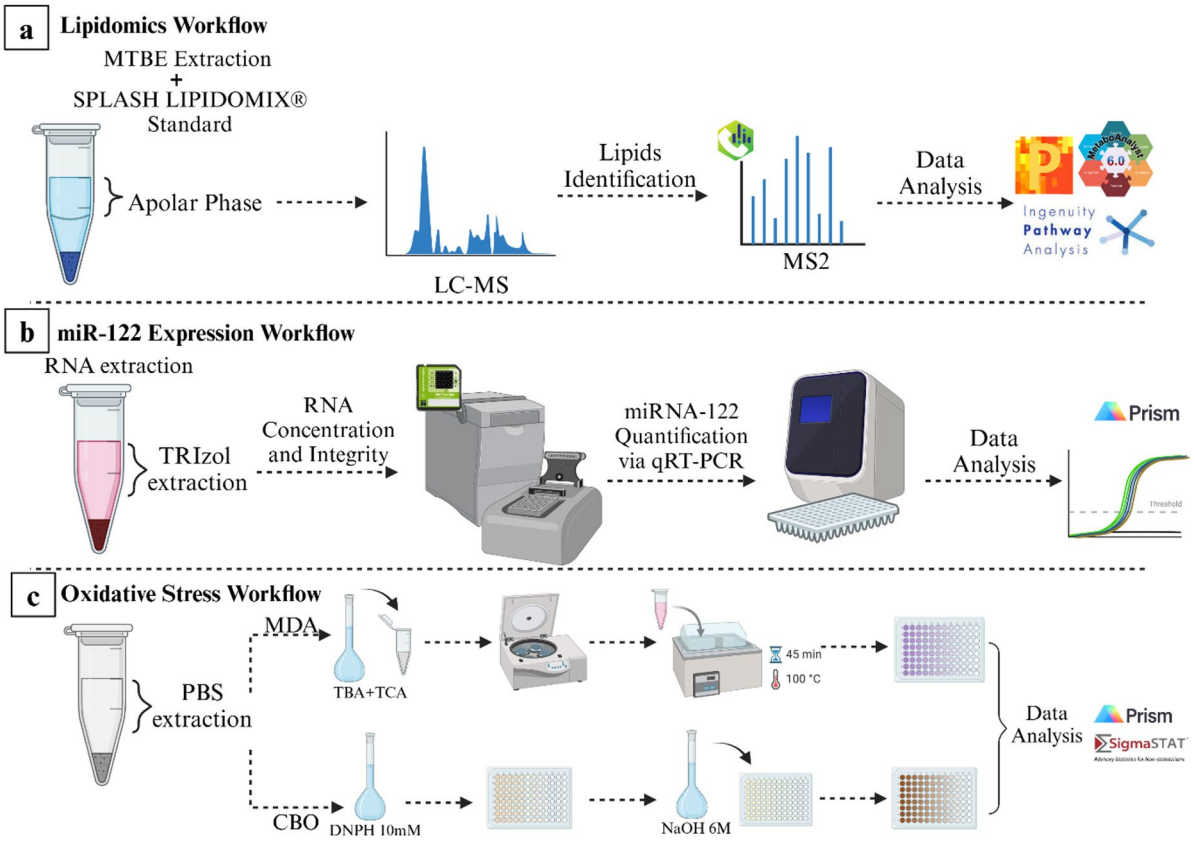

Fig. 6. Experimental workflow and data analysis (**a**) Lipidomics (**b**) miR-122 expression (**c**) Oxidative stress markers. CTRL: Control; HSF: high sugar-fat; ORY: gamma-oryzanol. MDA: Malondialdehyde. CBO: Protein Carbonylation. DNPH: 2,4-dinitrophenylhydrazine. NaOH: Sodium hydroxide. Created in BioRender. Siqueira, J. (2025) https://BioRender.com/q45q807.

Hepatic miR-122 expression

Total RNA, including miRNAs, was extracted from liver tissue using TRIzol® reagent (Invitrogen, USA), following the manufacturer's protocol. Samples were homogenized with ULTRA-TURRAX® (IKA, Germany) and processed through chloroform phase separation, isopropanol precipitation, ethanol washing, and resuspension in RNase-free water. RNA concentration and purity were assessed with a NanoDrop™ spectrophotometer (Thermo Scientific™), and integrity was evaluated using the Bioanalyzer® system (Agilent Technologies, USA) with RNA integrity number (RIN) confirmation. miRNA-122 expression was quantified using the TaqMan® MicroRNA Assays kit (#2245, Applied Biosystems, USA). RNA was DNase-treated, reverse-transcribed, and amplified by qPCR on a StepOnePlus™ system. U6 snRNA was used as the reference gene (#1973), and relative expression was calculated using the 2^−ΔΔCt method (Fig. 6B).

Hepatic oxidative stress

Tissues were homogenized with ice-cold Phosphate Buffered Saline solution (PBS, 1 mL, pH 7.4) using the ULTRA-TURRAX® T25 basic IKA® Werke Staufen/Germany, and centrifuged at 3500 rpm, at 4 °C for 10 min. A Spectra Max 190 microplate spectrophotometer (Molecular Devices®, Sunnyvale, CA, USA) was used to take the readings. To assess MDA levels (nmol/mg of protein), Thiobarbituric acid (TBA) at 0.67% was added to the supernatant (2:5; TBA: Supernatant) and followed by centrifugation at 3500 rpm for 10 min. Afterwards, the samples were heated for 45 min in a water bath and, after cooling, transferred to a 96-well plate for reading at 532 and 600 nm to calculate de MDA concentration from the molar extinction coefficient (1.56 × 105 M − 1 cm − 1)[50]. CBO (nmol of DNPH/mg of protein) was performed using 2,4-dinitrophenylhydrazine 10 mM (DNPH) and NaOH 6 M to detect by photometry proteins modified by carbonylation[51] (Fig. 6C).

Data analysis

Relative quantification was based on the determination of the peak intensities for each correctly identified lipid, which were then normalized by the intensity of the internal standard (ISTD) corresponding to each lipid class. The normalized peak intensities were exported to Microsoft Excel and used for statistical analysis and visualization using volcano plots generated in Perseus version 2.0.11 (https://maxquant.net/perseus/). Multivariate statistical analyses using Partial Least Squares Discriminant Analysis (PLS-DA) models were performed in MetaboAnalyst version 6.0 (https://www.metaboanalyst.ca), where discriminant lipids were selected based on Variable

Importance in Projection (VIP > 1). These analyses were conducted as predefined pairwise comparisons between groups (CTRL vs. HSF and HSF vs. HSF + ORY). Lipid molecules showing significant changes were annotated with unique identifiers from the Human Metabolome Database (HMDB, https://hmdb.ca) and integrated with the previously published proteomic dataset for network analysis using Ingenuity Pathway Analysis version 68,752,261 (IPA, QIAGEN Inc., USA, https://www.qiagenbioinformatics.com/products/ingenuity-pathway-analysis), which also relies on two-group comparisons. Differences among experimental groups in miR-122 expression and oxidative stress markers were assessed using one-way ANOVA followed by Tukey's post hoc test, with α set at 0.05. These statistical tests were performed using SigmaStat version 3.5 (Grafiti LLC, formerly Systat Software, https://www.grafiti.com/sigmastat), and all graphs were created in GraphPad Prism version 10 for Mac(https://www.graphpad.com).

Conclusion

This study demonstrated that ORY can modulate the expression of several classes of lipids in the liver, playing a significant role in networks involved in the pathophysiology of liver diseases. Notably, this is the first study to investigate the impact of ORY on integrated liver lipidomics/proteomics, providing novel insights into its potential therapeutic benefits. Additionally, ORY was shown to attenuate oxidative stress and regulate microRNA associated with lipid metabolism, reinforcing its multifaceted role in protecting against hepatic damage.

In conclusion, the integration of proteomic and lipidomic analyses provides a comprehensive understanding of the complex interactions between lipid metabolism, inflammation, and cellular viability in the context of MAFLD. The study highlights the potential therapeutic benefits of ORY, demonstrating its ability to modulate lipid profiles, reduce inflammatory pathways, oxidative stress and prevent the progression of hepatic steatosis. These findings suggest that ORY may play a significant role in mitigating obesity-related metabolic disorders and liver diseases. Further research is necessary to explore the precise molecular mechanisms and long-term effects of ORY, which could enhance its application as a natural therapeutic agent for preventing and managing MAFLD.

Data availability

All data included in this study is available upon request by contact with the corresponding author.

Received: 1 April 2025; Accepted: 31 October 2025
Published online: 02 December 2025

References

1. Malarkey, D. E., Johnson, K., Ryan, L., Boorman, G. & Maronpot, R. R. New insights into functional aspects of liver morphology. *Toxicol. Pathol.* **33**, 27–34 (2005).
2. Torre, P., Motta, B. M., Sciorio, R., Masarone, M. & Persico, M. Inflammation and Fibrogenesis in MAFLD: role of the hepatic immune system. *Front. Med. (Lausanne)* **8**, 781567 (2021).
3. Ramazani, E., Akaberi, M., Emami, S. A. & Tayarani-Najaran, Z. Biological and Pharmacological effects of Gamma-oryzanol: an updated review of the molecular mechanisms. *Curr. Pharm. Des.* **27**, 2299–2316 (2021).
4. Francisqueti-Ferron, F. V. et al. Preventive effect of Gamma-Oryzanol on physiopathological process related to nonalcoholic fatty liver disease in animals submitted to high Sugar/Fat diet. *Livers* **2**, 146–157 (2022).
5. Siqueira, J. S. et al. Proteomic study of gamma-oryzanol preventive effect on a diet-induced non-alcoholic fatty liver disease model. *J. Nutr. Biochem.* **127**, 109607 (2024).
6. Jani, S. et al. Distinct mechanisms involving diacylglycerol, ceramides, and inflammation underlie insulin resistance in oxidative and glycolytic muscles from high fat-fed rats. *Sci. Rep.* **11**, 19160 (2021).
7. Gruevska, A. et al. Spatial lipidomics reveals sphingolipid metabolism as anti-fibrotic target in the liver. *Metabolism* **168**, 156237 (2025).
8. Peng, K. Y. et al. Mitochondrial dysfunction-related lipid changes occur in nonalcoholic fatty liver disease progression. *J. Lipid Res.* **59**, 1977–1986 (2018).
9. Noeman, S. A., Hamooda, H. E. & Baalash, A. A. Biochemical study of oxidative stress markers in the Liver, kidney and heart of high fat diet induced obesity in rats. *Diabetol. Metab. Syndr.* **3**, 17 (2011).
10. Csak, T. et al. microRNA-122 regulates hypoxia-inducible factor-1 and vimentin in hepatocytes and correlates with fibrosis in diet-induced steatohepatitis. *Liver Int.* **35**, 532–541 (2015).
11. Wu, G. et al. MicroRNA-122 inhibits lipid droplet formation and hepatic triglyceride accumulation via Yin Yang 1. *Cell. Physiol. Biochem.* **44**, 1651–1664 (2017).
12. Paluschinski, M. et al. Differential modulation of miR-122 transcription by TGFβ1/BMP6: implications for nonresolving inflammation and hepatocarcinogenesis. *Cells* **12**, 1955 (2023).
13. Cong, S. et al. Integrative proteomic and lipidomic analysis of Kaili sour Soup-mediated Attenuation of high-fat diet-induced nonalcoholic fatty liver disease in a rat model. *Nutr. Metab. (Lond).* **18**, 26 (2021).
14. Vvedenskaya, O. et al. Nonalcoholic fatty liver disease stratification by liver lipidomics. *J. Lipid Res.* **62**, 100104 (2021).
15. Musso, G., Cassader, M., Paschetta, E. & Gambino, R. Bioactive lipid species and metabolic pathways in progression and resolution of nonalcoholic steatohepatitis. *Gastroenterology* **155**, 282–302e8 (2018).
16. Liu, Z., Liu, X., Ma, Z. & Guan, T. Phytosterols in rice bran and their health benefits. *Front. Nutr.* **10**, 1287405 (2023).
17. Wang, J. et al. Recent updates on targeting the molecular mediators of NAFLD. *J. Mol. Med.* **101**, 101–124 (2023).
18. Topham, M. K. Diacylglycerol Kinases and Phosphatidic Acid Phosphatases. in *Encyclopedia of Biological Chemistry* 659–663Elsevier, https://doi.org/10.1016/B978-0-12-378630-2.00409-6(2013).
19. Mouskeftara, T., Deda, O., Papadopoulos, G., Chatzigeorgiou, A. & Gika, H. Lipidomic analysis of liver and adipose tissue in a High-Fat Diet-Induced Non-Alcoholic fatty liver disease mice model reveals alterations in lipid metabolism by weight loss and aerobic exercise. *Molecules* **29**, 1494 (2024).
20. Syed-Abdul, M. M. Lipid metabolism in Metabolic-Associated steatotic liver disease (MASLD). *Metabolites* **14**, 12 (2023).
21. Samuel, V. T. et al. Inhibition of protein kinase Cε prevents hepatic insulin resistance in nonalcoholic fatty liver disease. *J. Clin. Invest.* **117**, 739–745 (2007).
22. Zhang, L., Mu, J., Meng, J., Su, W. & Li, J. Dietary phospholipids alleviate Diet-Induced obesity in mice: which fatty acids and which Polar head. *Mar. Drugs.* **21**, 555 (2023).

23. Cole, L. K., Vance, J. E. & Vance, D. E. Phosphatidylcholine biosynthesis and lipoprotein metabolism. *Biochim. Et Biophys. Acta (BBA) - Mol. Cell. Biology Lipids*. **1821**, 754–761 (2012).
24. Qiu, Y. Y., Zhang, J., Zeng, F. Y. & Zhu, Y. Z. Roles of the peroxisome proliferator-activated receptors (PPARs) in the pathogenesis of nonalcoholic fatty liver disease (NAFLD). *Pharmacol. Res.* **192**, 106786 (2023).
25. Francisqueti, F. V. et al. Gamma Oryzanol treats Obesity-Induced kidney injuries by modulating the adiponectin receptor 2 / PPAR- α axis. *Oxid. Med. Cell. Longev.* **2018**, 1–9 (2018).
26. Green, C. D., Maceyka, M., Cowart, L. A. & Spiegel, S. Sphingolipids in metabolic disease: the good, the bad, and the unknown. *Cell. Metab.* **33**, 1293–1306 (2021).
27. Mitsutake, S. et al. Dynamic modification of sphingomyelin in lipid microdomains controls development of Obesity, fatty Liver, and type 2 diabetes. *J. Biol. Chem.* **286**, 28544–28555 (2011).
28. Iqbal, J., Walsh, M. T., Hammad, S. M. & Hussain, M. M. Sphingolipids and lipoproteins in health and metabolic disorders. *Trends Endocrinol. Metabolism*. **28**, 506–518 (2017).
29. Galicia-Moreno, M. et al. Behavior of oxidative stress markers in alcoholic liver cirrhosis patients. *Oxid. Med. Cell Longev.* **2016**, 9370565 (2016).
30. Shi, S., Wang, L., van der Laan, L. J. W., Pan, Q. & Verstegen, M. M. A. Mitochondrial dysfunction and oxidative stress in liver transplantation and underlying diseases: new insights and therapeutics. *Transplantation* **105**, 2362–2373 (2021).
31. Hochreuter, M. Y., Dall, M., Treebak, J. T. & Barrès, R. MicroRNAs in non-alcoholic fatty liver disease: progress and perspectives. *Mol. Metab.* **65**, 101581 (2022).
32. Lu, R. H. et al. The function of miR-122 in the lipid metabolism and immunity of grass carp (Ctenopharyngodon idellus). *Aquac Rep.* **17**, 100401 (2020).
33. Moore, K. J., Rayner, K. J., Suárez, Y. & Fernández-Hernando, C. The role of MicroRNAs in cholesterol efflux and hepatic lipid metabolism. *Annu. Rev. Nutr.* **31**, 49–63 (2011).
34. Matheson, J., Zhou, X. M. M., Bourgault, Z. & Le Foll, B. Potential of fatty acid amide hydrolase (FAAH), monoacylglycerol lipase (MAGL), and Diacylglycerol lipase (DAGL) enzymes as targets for obesity treatment: A narrative review. *Pharmaceuticals* **14**, 1316 (2021).
35. Nesto, R. W. & Mackie, K. Endocannabinoid system and its implications for obesity and cardiometabolic risk. *Eur. Heart J. Supplements*. **10**, B34–B41 (2008).
36. Auguet, T., Berlanga, A., Guiu-Jurado, E. & Porras, J. A. Molecular pathways in non-alcoholic fatty liver disease. *Clin. Exp. Gastroenterol.* https://doi.org/10.2147/CEG.S62831 (2014).
37. Mallat, A., Teixeira-Clerc, F. & Lotersztajn, S. Cannabinoid signaling and liver therapeutics. *J. Hepatol.* **59**, 891–896 (2013).
38. Minatel, I., Francisqueti, F., Corrêa, C. & Lima, G. Antioxidant activity of γ-Oryzanol: A complex network of interactions. *Int. J. Mol. Sci.* **17**, 1107 (2016).
39. Singh, A. B., Kan, C. F. K., Kraemer, F. B., Sobel, R. A. & Liu, J. Liver-specific knockdown of long-chain acyl-CoA synthetase 4 reveals its key role in VLDL-TG metabolism and phospholipid synthesis in mice fed a high-fat diet. *Am. J. Physiology-Endocrinology Metabolism*. **316**, E880–E894 (2019).
40. Ruiz-Blázquez, P., Pistorio, V., Fernández-Fernández, M. & Moles, A. The multifaceted role of cathepsins in liver disease. *J. Hepatol.* **75**, 1192–1202 (2021).
41. Miller, A. F. Superoxide dismutases: ancient enzymes and new insights. *FEBS Lett.* **586**, 585–595 (2012).
42. El Hadi, H., Di Vincenzo, A., Vettor, R. & Rossato, M. Relationship between heart disease and liver disease: A Two-Way street. *Cells* **9**, 567 (2020).
43. Bauernfeind, F. G. et al. Cutting edge: NF-κB activating pattern recognition and cytokine receptors license NLRP3 inflammasome activation by regulating NLRP3 expression. *J. Immunol.* **183**, 787–791 (2009).
44. Randomized, A. Double blind clinical study to assess the effects of a Gamma-oryzanol-enriched rice Bran oil on lipid profile in the hypercholesterolemic patients. *J. Med. Assoc. Thai.* **104**, S64–S69 (2021).
45. Juricic, H. et al. Biochemical, Biological, and clinical properties of γ-Oryzanol. *Antioxidants* **14**, 1099 (2025).
46. Francisqueti-Ferron, F. V. et al. Gamma-oryzanol reduces renal inflammation and oxidative stress by modulating AGEs/RAGE axis in animals submitted to high sugar-fat diet. *Brazilian J. Nephrol.* **43**, 460–469 (2021).
47. Garcia, J. L. et al. Rice (Oryza sativa L.) Bran preserves cardiac function by modulating pro-inflammatory cytokines and redox state in the myocardium from obese rats. *Eur. J. Nutr.* **61**, 901–913 (2022).
48. Mattei, L. et al. Antioxidant and anti-inflammatory properties of gamma- Oryzanol attenuates insulin resistance by increasing GLUT- 4 expression in skeletal muscle of obese animals. *Mol. Cell. Endocrinol.* **537**, 111423 (2021).
49. Zoanni, B. et al. Lipidome investigation of carnosine effect on nude mice skin to prevent UV-A damage. *Int. J. Mol. Sci.* **24**, 10009 (2023).
50. Uchiyama, M. & Mihara, M. Determination of malonaldehyde precursor in tissues by thiobarbituric acid test. *Anal. Biochem.* **86**, 271–278 (1978).
51. Mesquita, C. S. et al. Simplified 2,4-dinitrophenylhydrazine spectrophotometric assay for quantification of carbonyls in oxidized proteins. *Anal. Biochem.* **458**, 69–71 (2014).

Acknowledgements

The authors acknowledge Unitech OMICs at the University of Milan for producing the raw mass spectrometry data, National Council for Scientific and Technological Development – CNPq [grant number 310614/2020-1] and São Paulo Research Foundation –FAPESP [grant number 2018/15294-3]. Some figures in this paper were created with BioRender.com and the corresponding publication and licensing rights were obtained (Siqueira, J. (2025) https://BioRender.com/q45q807; https://BioRender.com/r37r762).

Author contributions

J.S.S. and T.L.N.P. wrote the original draft of the manuscript. J.S.S. G.Ai., J.C., H.J.B.C.S., T.L.N.P, and A.D. contributed to the methodology. J.S.S., C.R.C., F.V.F.F., M.C., G.Al., and A.D. contributed to the conceptualization of the study. J.S.S., G.Ai., E.O.L and A.D. contributed to data curation. J.S.S. and C.R.C. acquired funding. C.R.C. and A.D. supervised the study. C.R.C., M.C., and A.D. were responsible for project administration. A.D. reviewed and edited the manuscript. All authors reviewed and approved the final version of the manuscript.

Funding

This work was supported by the São Paulo Research Foundation –FAPESP [grant numbers 2022/16108-4, 2015/10626-0]; Coordenação de Aperfeiçoamento de Pessoal de Nível Superior – CAPES [grant number 88887.891854/2023-00]; National Council for Scientific and Technological Development – CNPq [306640/2023-6].

Declarations

Competing interests
The authors declare no competing interests.

Additional information
Supplementary Information The online version contains supplementary material available at https://doi.org/10.1038/s41598-025-26929-7.

Correspondence and requests for materials should be addressed to J.S.S. or E.O.L.

Reprints and permissions information is available at www.nature.com/reprints.

Publisher's note Springer Nature remains neutral with regard to jurisdictional claims in published maps and institutional affiliations.

Open Access This article is licensed under a Creative Commons Attribution-NonCommercial-NoDerivatives 4.0 International License, which permits any non-commercial use, sharing, distribution and reproduction in any medium or format, as long as you give appropriate credit to the original author(s) and the source, provide a link to the Creative Commons licence, and indicate if you modified the licensed material. You do not have permission under this licence to share adapted material derived from this article or parts of it. The images or other third party material in this article are included in the article's Creative Commons licence, unless indicated otherwise in a credit line to the material. If material is not included in the article's Creative Commons licence and your intended use is not permitted by statutory regulation or exceeds the permitted use, you will need to obtain permission directly from the copyright holder. To view a copy of this licence, visit http://creativecommons.org/licenses/by-nc-nd/4.0/.

© The Author(s) 2025